COMPDYN 2011
III ECCOMAS Thematic Conference on
Computational Methods in Structural Dynamics and Earthquake Engineering
M. Papadrakakis, M. Fragiadakis, V. Plevris (eds.)
Corfu, Greece, 25–28 May 2011

FRAGILITY ASSESSMENT OF RC FRAMES COLLAPSE CAPACITY

Ilias A. Gkimousis[1], Vlasis K. Koumousis[1]

[1]Institute of Structural Analysis & Aseismic Research
National Technical University of Athens
Zographou Campus GR-15780, Athens, Greece
iliasgkim@hotmail.com, vkoum@central.ntua.gr

Keywords: Incremental Dynamic Analysis, Fragility Curves, Probability of Collapse, Redundancy, Stiffness Distribution, Strong Column-Weak Beam ratio

Abstract. *The inelastic behavior of reinforced concrete structures subjected to a number of strong motion excitations of escalated Intensity Measure (IM) and monitoring of characteristic Engineering Demand Parameters (EDPs) of the structure for all these different instances is presented. This provides the necessary data to estimate the overall response of a structure at a particular site of specified seismic hazard and constitutes the framework of Incremental Dynamic Analysis (IDA). In this, generation of data regarding capacity and demand evolves following a lognormal distribution while the corresponding cumulative distribution function is used to define the corresponding fragility curves. This analysis facilitates further the deduction of statistically sound estimates of the measured parameters. The hysteretic inelastic response of reinforced concrete members, i.e. beams and columns designed on the basis of Eurocodes is of primal importance. The Bouc-Wen model, as implemented in "Plastique" code is considered following the IDA procedure, the parameters of which are established based on existing experimental data. Through this modelling, a series of plane frames of different number of spans and storeys designed in a similar manner is investigated. Also, the effect of some general design code provisions on collapse capacity of these frames, such as stiffness distribution along height and strong column- weak beam ratio, are examined. Numerical results are presented and their corresponding fragility curves are derived. Interesting features are revealed, regarding the effect of each alternative design on collapse capacity, which often deviate from collapse predictions made using the static pushover analysis.*

1 INTRODUCTION

One of the main objectives of current earthquake-resistant design codes is to ensure increased levels of safety commencing with protection of human life during strong earthquakes, while reducing damage - repair cost for small and medium excitations for new and existing structures. This constitutes the framework of Performance Based Earthquake Engineering (PBEE) by defining performance levels which correspond to different damage situations. The level of collapse prevention for example, demands certain probability of collapse that does not exceed the acceptable limits set for this purpose. However, at the moment, code provisions are deterministic in nature, as they are based on return periods relating seismic excitation with specific levels of damage.

Hence, it is important to establish these probabilities and follow design methods that statistically ensure the non exceedance of the specified damage state. The Incremental Dynamic Analysis (IDA) [1, 2] addresses this issue by calculating statistical data in terms of Intensity Measure (IM) and Engineering Demand Parameters (EDPs). This is followed by a statistical analysis of the outcome and the evaluation of fragility curves [3, 4]. This procedure is capable of revealing significant probabilistic evidence of structural behaviour by defining relation between probability of collapse and ground motion IM. If fragility curves are combined with seismic hazard data from a certain region of interest, that combine the same IM with the seismic hazard, the Mean Annual Frequency (MAF) of exceeding a performance state is derived for the particular seismic hazard site.

In this paper the aforementioned methodology is used to assess collapse capacity of Reinforced Concrete plane frames designed following different considerations. It should be noted that these frames are centreline models of 3D symmetrical structures with equal inertia characteristics and fixed supports. More specifically, this study concentrates on the performance state of dynamic collapse by examining the effect of geometrical and structural frame parameters on the probability that a collapse event occurs.

2 ANALYTICAL PROCEDURE

2.1 Implementing IDA

In order to perform nonlinear elastoplastic dynamic analysis following the IDA method, the ‘’Plastique’’ [5] program was used which employs the phenomenological Bouc-Wen hysteretic model, the parameters of which were defined as described in [6]. To establish more realistic results as the structure approaches collapse where large displacements, i.e. P-Δ effects, become significant and they were introduced according to [7]. This is a simple, approximate, non-iterative technique, where lateral forces are introduced to each storey level due to the overturning moments caused by the movement of diaphragm masses.

As far as IDA is concerned, as the scalar, escalated intensity measure (IM) the 1st eigenmode spectral acceleration with 5% viscous damping Sa (T1, 5%) was selected. Respectively, the engineering demand parameter (EDP) that measures demand on different levels of structural deterioration is the maximum interstorey drift ratio. To save computational time the haunt & fill algorithm as the method to trace IDA curves, after repeated runs, was selected [2]. This was parameterized properly to achieve as much accuracy as possible in the region of dynamic instability. Twenty accelerograms were selected for the analysis, corresponding to major earthquakes in California and they are listed in [2, 8]. They consist of relatively large magnitude excitations, moderate distances from fault, so as to avoid pulse excitations and near field effects [9]. In Figure 1, the median and the 84% percentile response spectra for all twenty excitations are presented. The only source of uncertainty used in this

study is the record to record variability (aleatory uncertainty) which is sensitive to the dispersion of spectra in the region of structure's 1st eigenperiod. For the selected ground motions this dispersion in their spectral accelerations is computed in terms of logarithmic standard deviation through equation (1) and the final graph is presented in Figure 2.

$$\sigma_{\ln,y} = \ln\left(\frac{y_{84}}{y_{50}}\right) \tag{1}$$

where, y_{50} are the median spectral values while y_{84} are the 84% percentile spectral values for a given eigenperiod.

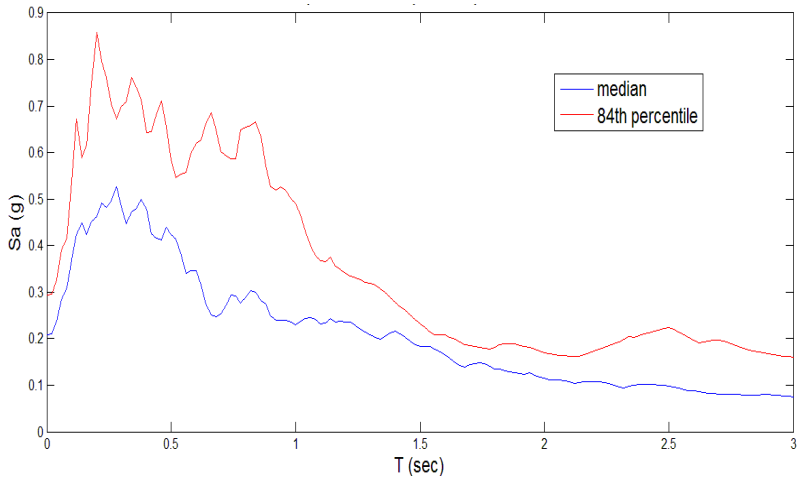

Figure 1: Median and 84% percentile response spectra for all twenty earthquakes

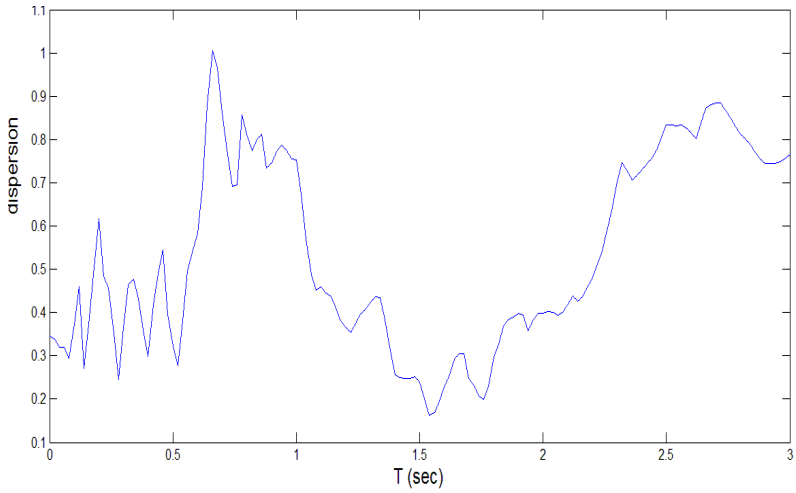

Figure 2: Dispersion of twenty acceleration spectra for the eigenperiods of interest.

2.2 Statistical evaluation

After performing the computationally demanding IDA, some very important features usually emerge with the proper statistical evaluation of the outcome. The statistical sample in this work consists of twenty spectral accelerations (Sa_c) where dynamic collapse occurred. Collapse is considered to happen, when a global or local collapse mechanism is formed, or when maximum interstorey drift ratio exceeds the value of 12%. In order to pursue analytical calculations, a lognormal distribution is fitted to the data and by calculating its cumulative

distribution function (CDF) a collapse fragility curve, based on the IM approach [3, 4], is derived as follows:

$$P[Sa_c \le Sa] = \Phi\left[\frac{1}{\beta_{Sa,c}} \ln(\frac{Sa}{n_{Sa,c}})\right] \tag{2}$$

where, $\beta_{Sa,c}$ is the standard deviation of the natural logarithm, while $n_{Sa,c}$ is the lognormal median of the data.

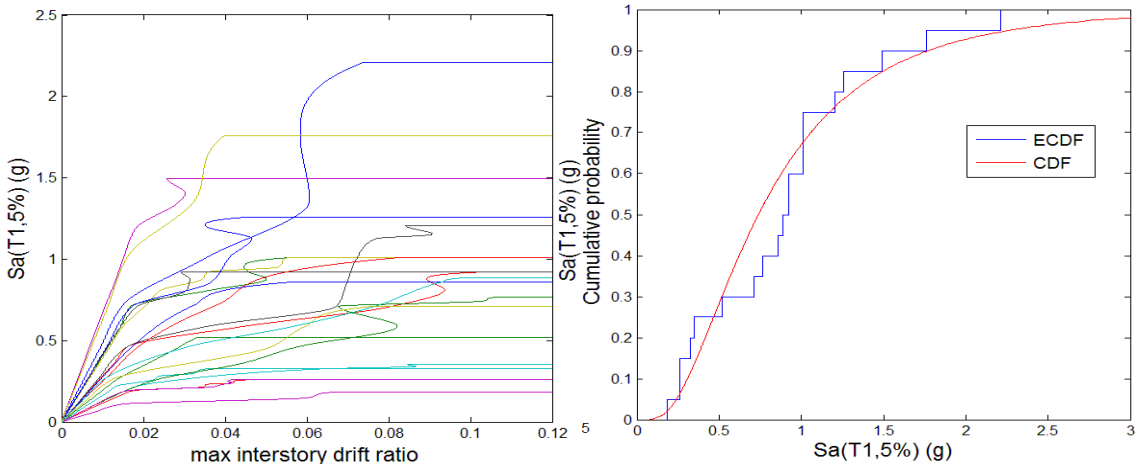

(a) (b)

Figure 3: a) All 20 IDA curves, b) Corresponding empirical and analytical fragility curves

The above described steps are presented in Figure 3, for the case of a 6-storey, 2-bay plane RC frame with first eigenfrequency, T_1= 0.639 sec. In the figure, the lognormal distribution, fitted to the data, is presented and consists the fragility curve for this frame.

Furthermore, in the literature several indices are defined that can be used to quantify the stochastic nature of fragility. To determine the most representative ones, a Probabilistic Seismic Hazard Analysis (PSHA) for the seismic site of interest is required, that provides the necessary hazard spectra and hazard curves. This data, when combined with fragility curves, can reveal the very important feature of how rarely a structure collapses when it is subjected to spectral accelerations that are possible to occur in the specific geographical region. This measure is the mean annual frequency (MAF) of collapse and its inverse is the collapse return period of the structure. In this study, the hazard curves that were implemented in the procedure are referred to the IM and are given in [10]. The indices used [11] are the median collapse spectral acceleration $(Median\,(Sa_c))$, the probability of collapse for the earthquake with probability of occurrence 10%/50 years $(P_{C|10\%/50y})$, the Margin Against Collapse (MAC) for the 10%/50 years earthquake (eq. 3) and the MAF of collapse (eq. 4). Also, the dispersion of structural behaviour according to different seismic excitations can be described through the standard deviation of the natural logarithm of the data $\left(\sigma_{\ln}\right)$.

$$MAC_{10\%/50\,years} = \frac{Median\,(Sa_c)}{Sa_{10\%/50\,years}} \tag{3}$$

where $Sa_{10\%/50\,years}$ is given in the hazard spectrum and defines the spectral acceleration that is expected to occur when the earthquake with probability of occurrence 10% in 50 years strikes.

$$MAF = \lambda_c = \int_0^{\infty} F_{C,Sa,c}(x) \left| d\lambda_{Sa}(x) \right| \tag{4}$$

where $F_{C,Sa,c}(x)$ is the collapse fragility curve and $\lambda_{Sa}(x)$ is the ground motion hazard curve.

3 EFFECT OF DESIGN CRITERIA IN THE COLLAPSE CAPACITY OF RC FRAMES

3.1 Effect of the number of bays and storeys

In Figure 4, eight plane RC frames of 3 and 6 storeys have been designed according to Greek codes, with number of bays ranging from 1 to 4. In order to facilitate comparison they retain the same reinforcement in the interior and exterior columns respectively.

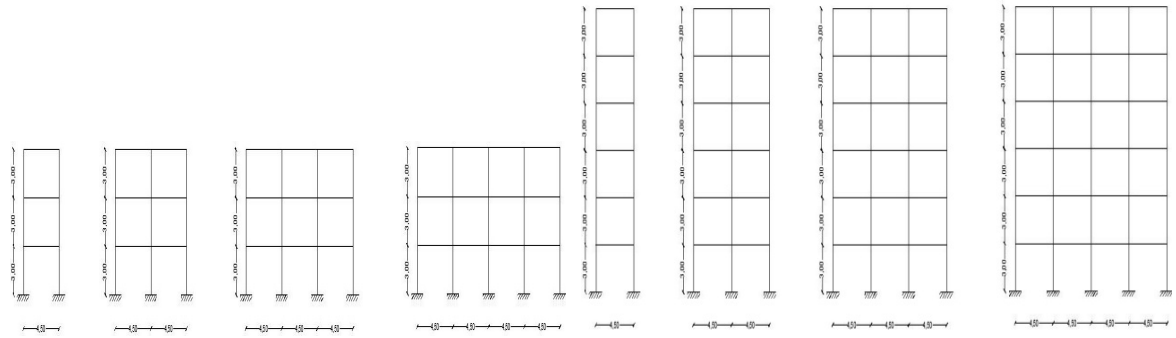

(a) (b)

Figure 4: a) 3 storey frames, b) 6 storey frames

Column sections (m)	Beam sections (m)	Bay length (m)	Storey height (m)
0.25x 0.25	0.30x0.20	4.50	3.00

Table 1: Plane frames geometrical features

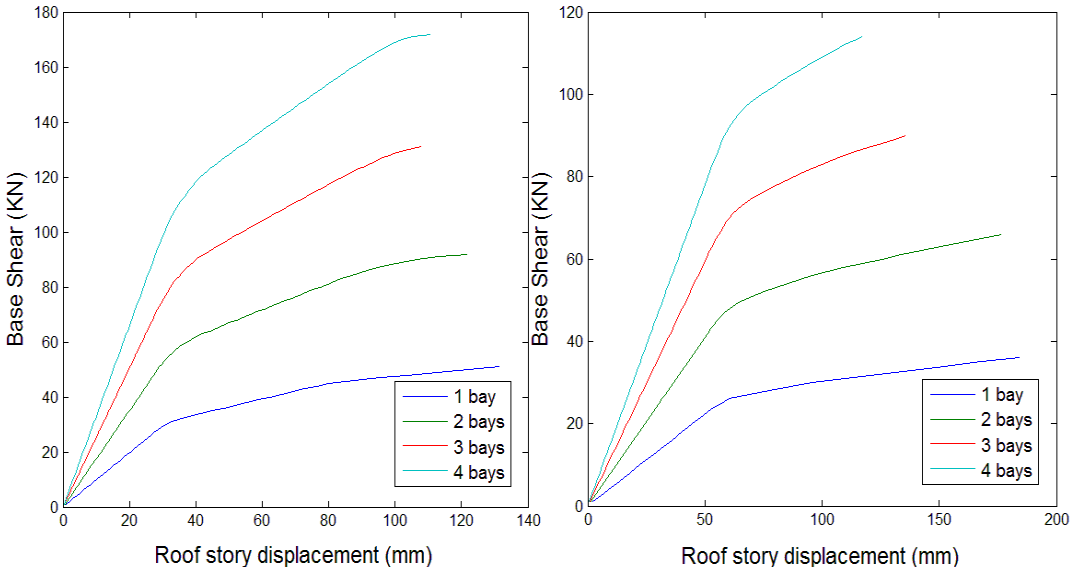

(a) (b)

Figure 5: a) Pushover curves for 3 story frames, b) Pushover curves for 6 story frames

Next, the static pushover results with triangular lateral force distribution are displayed in Figure 5. The general trend is that, as the number of bays increases, redundancy also increases and the greater possibility for force redistribution exists, resulting into higher capacity [13].

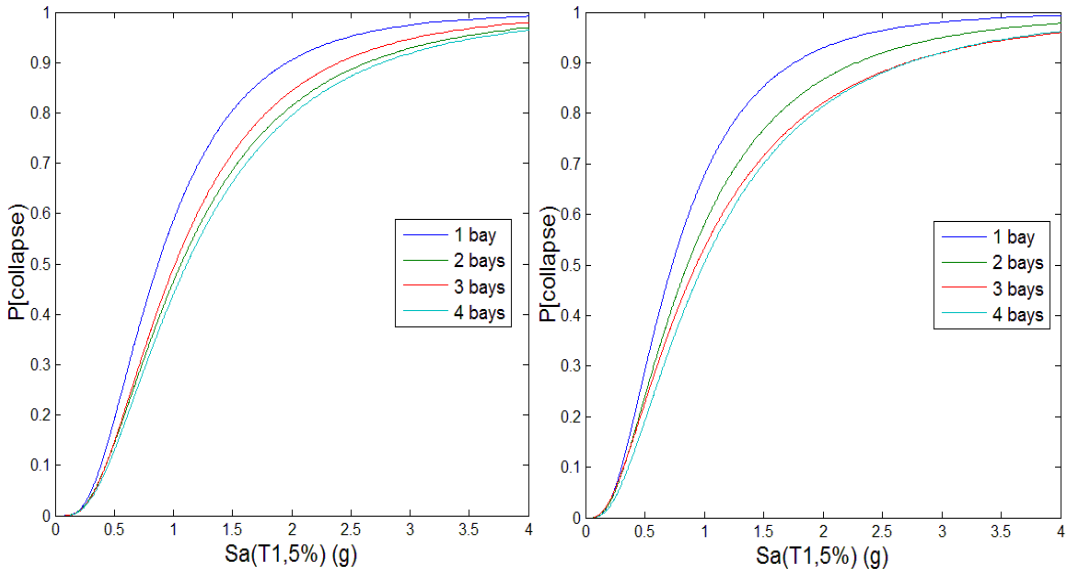

(a) (b)

Figure 6: a) Collapse fragility curves for 3 storey frames, b) Collapse fragility curves for 6 storey frames

The same frames are analysed following the IDA method. Collapse fragility curves are produced and they are presented in Figure 6. In Table 2 the probabilistic indices for collapse estimation have been calculated, together with measures of deformation such as the median interstorey drift ratio (IDR) and the median roof drift ratio (RDR). It is important to notice that the results are meant only for comparison between the different frames of the analysis as they appear inadequate to withstand the strong earthquakes of California, as they are poorly designed with the minimum code reinforcement.

Storeys	Bays	T1(sec)	Median (Sa_C)	$\sigma_{\ln}$	$P_{C\|10\%/50y}$	MAC	λ_C	Median (IDR)	Median (RDR)
3	1	0.324	0.87	0.63	74%	0.67	0.0121	0.031	0.023
	2	0.349	1.06	0.70	61%	0.82	0.0098	0.079	0.053
	3	0.357	1.02	0.67	64%	0.78	0.0103	0.054	0.041
	4	0.362	1.12	0.71	59%	0.86	0.0093	0.089	0.054
6	1	0.650	0.70	0.68	75%	0.63	0.0100	0.045	0.022
	2	0.693	0.86	0.76	65%	0.75	0.0086	0.080	0.035
	3	0.708	0.93	0.82	60%	0.81	0.0076	0.080	0.038
	4	0.717	1.00	0.77	57%	0.87	0.0068	0.076	0.040

Table 2: Collapse capacity quantification for all RC frames

A basic difference between pushover and IDA is that in the case of 3-storey frames collapse capacity does not increase with the increase of the number of bays. More specifically, the 2-bay frame exhibits smaller probability of collapse for the 10%/50 years earthquake and smaller MAF of collapse than the 3-bay frame. Comparing the two different groups of frames, the 6-storey frames result into larger dispersion of the results due to the fact that their eigenperiods represent larger spectral dispersion according to Figure 2. Also, median collapse spectral acceleration (Sa_c) takes smaller values for the 6-storey frames. Although it results

that with the increase of frame height collapse capacity decreases, which is logical as P-Δ effects becomes important and also higher axial load in columns causes their ductility to diminish, this statement can't be generalised due to the limited sample of the current study. In contrast, the MAF of collapse for the 6-storey frames seems to be smaller, meaning larger collapse return periods, since smaller spectral accelerations are expected to appear in larger eigenperiods. The context of table 2 is displayed graphically in Figure 7.

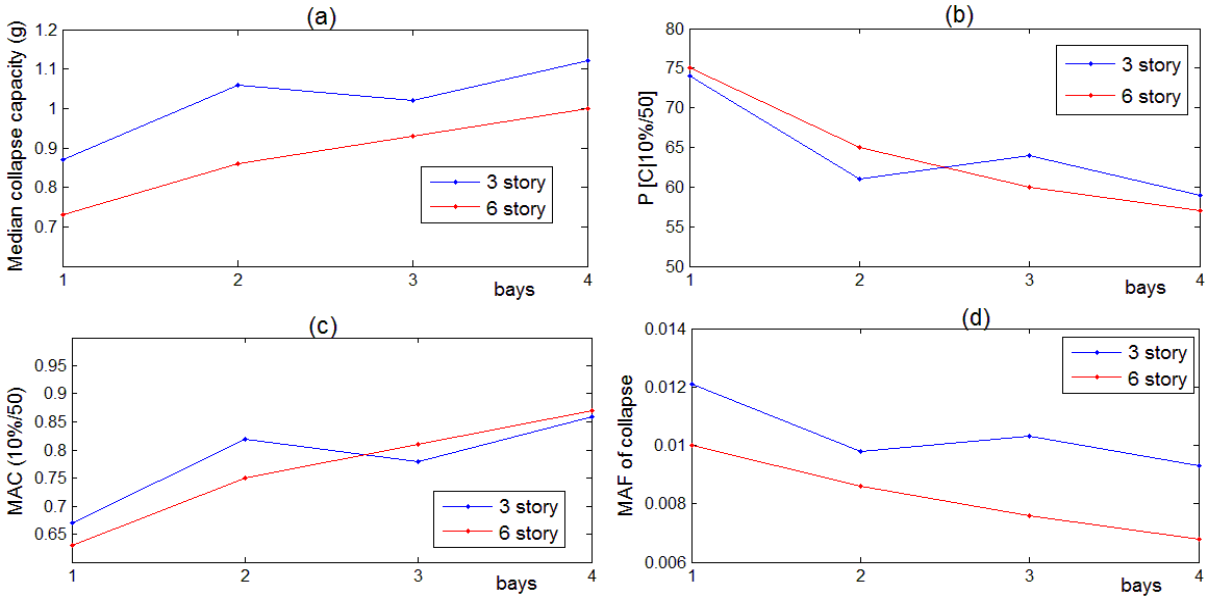

Figure 7: Effect of the number of bays and storeys in frames collapse capacity. a) Median collapse capacity, b) Probability of collapse for the 10%50 years earthquake, c) MAC for the 10%/50 years earthquake, d) MAF of collapse

The results of the last 2 columns in table 2 that refer to deformations are presented in Figure 8.

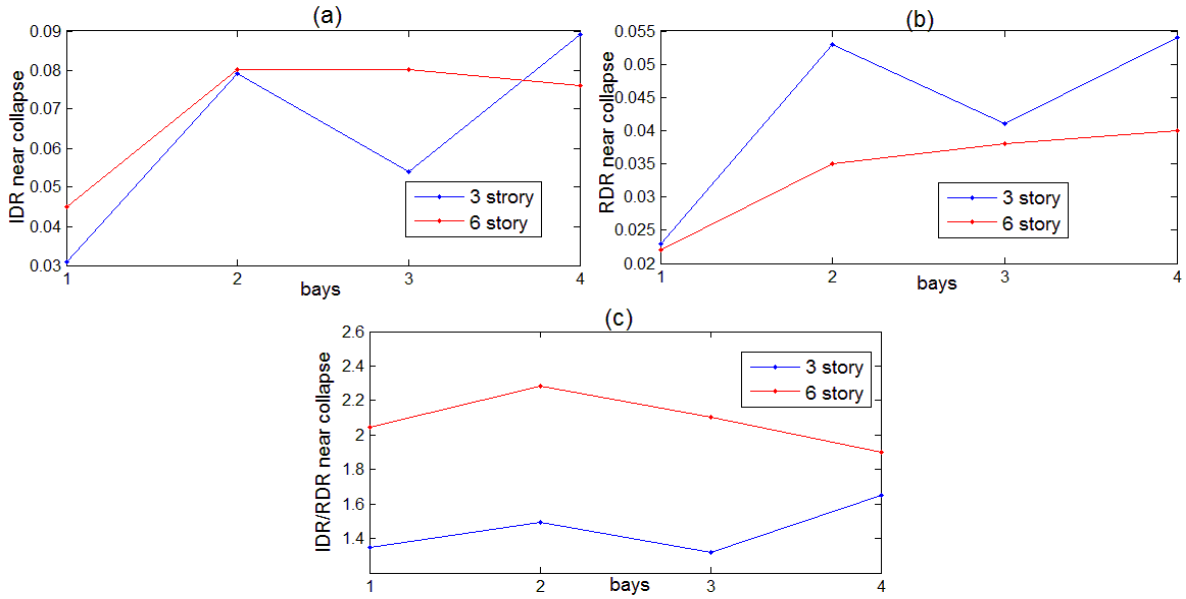

Figure 8: Effect of the number of bays and storeys in frames displacements near collapse. a) Interstorey drift ratio (IDR), b) Roof drift ratio (RDR), c) IDR/RDR

In Figure 8c, IDR/RDR ratio depicts the degree of damage accumulation in a few storeys. As the ratio becomes bigger, like in 6-storey frames, it is portrayed that damage is localized in a few storeys of the building, while in 3-storey frames damage is almost equally distributed along the height. Generally, 1-bay frames develop smaller displacements and for 6-storey frames they seem to stabilize when more bays are added. Also, 6-storey frames don't exhibit as large demands in displacements as the 3-storey frames, for the same reasons that collapse capacity in terms of spectral accelerations decreases, as it was mentioned.

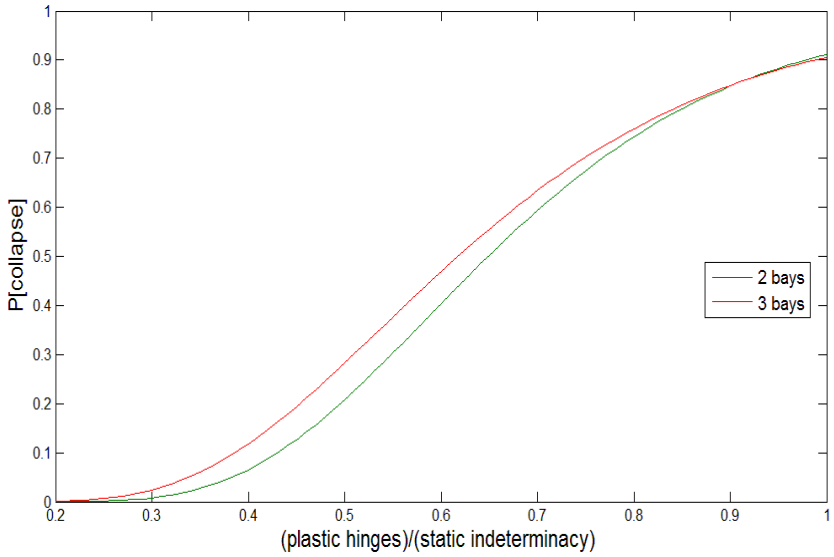

Figure 9: Number of plastic hinges involved in collapse for 2-bays and 3-bays frames

In Figures 7 and 8 it is evident that for 3-storey frames, although it was expected to develop higher strength against collapse than the 2-bay frames, the opposite happens. It is probable that this feature is caused by local collapse mechanisms that don't allow the structure to take advantage of its full redundancy. To elaborate more on this fact, the measure of structural redundancy that was given by Bertero and Bertero [14] was investigated. This measure is the number of plastic hinges n that yield or fail at structural members ends until total collapse. So, in each single record IDA run where collapse is detected, the number of formed plastic hinges is recorded. This number is divided by the number of static indeterminacy of the structure to determine the redundancy ratio. Thus, a statistical set with 20 values is formed and the results are presented in the form of a cumulative distribution function in Figure 9. It is clear that the 3-bay frame stays behind in consuming its full redundancy for a specific probability of collapse. Therefore, for a given probability of collapse, in the 3-bay frame the redundancy ratio, that expresses the cross sections that have yielded or failed, is smaller than the redundancy ratio in the 2-bay frame respectively, a fact that reveals the probabilistic nature of structural redundancy as related to seismic loading.

The nonlinear modelling of structures with the notion of plastic hinge formation reveals the estimated form of collapse. For every collapse mechanism identified in each single record IDA, the number of storeys involved in the mechanism is recorded and the results are shown in Table 3. A particular storey is assumed to participate in the collapse mechanism when at least one plastic hinge appears on its columns or on its beams.

Geometrical features		Percentages of observed plastic hinges						
Storeys	Bays	Storeys 1-1 (%)	Storeys 1-2 (%)	Storeys 1-3(%)	Storeys 1-4(%)	Storeys 1-5(%)	Storeys 1-6(%)	Percentages of storeys involved in collapse (%)
3	1	0	40	60	0	0	0	87
	2	0	25	75	0	0	0	92
	3	0	25	75	0	0	0	92
	4	0	30	70	0	0	0	90
6	1	0	0	15	15	45	25	80
	2	0	0	15	15	35	35	82
	3	0	0	10	30	35	25	79
	4	0	0	5	30	40	25	81

Table 3: Storeys involved in collapse mechanism for each frame

For example in 6-storey, 2-bay frame, plastic hinges are formed in the first 3 storeys in 15% of all the occasions, in the first 4 storeys in 15%, in the first 5 storeys in 35% and all storeys are involved in collapse mechanism in 35% of all the occasions. Also, the total percentage of storeys where plastic hinges are formed in their beams or columns is 82%. Generally, from Table 3 it is observed that the distribution of plastic hinges along height is not influenced by the number of bays and that there is a tendency for concentration of damage in higher floors. There is no case of first storey mechanism for the 3-storey frames, not first or second storey mechanism for 6-storey frames. The involvement of fifth and sixth storey is significant, since flexural strength of columns is about 3 times bigger than flexural strength of beams causing the beams in upper floors to yield faster. Finally, percentages of storeys involved in collapse for 6-storey frames are clearly smaller, a fact that comes in agreement with Figure 8(c). Hence, it is evident from a different perceptive that damage concentrates in few storeys in the case of the 6-storey frames.

3.2 Effect of stiffness distribution along height

To examine the effect of stiffness distribution along the height in RC frames collapse capacity, 2 different designs of the 6-storey 2-bay frames have been analysed. The study refers to normal, moment resisting frames, mass is considered equal in all storeys and distribution of stiffness between 2 consecutive storeys doesn't exceed 60%. Also, the same moment of inertia is attributed to the same floor's members, as all beams and columns have the same geometrical properties. In order to quantify stiffness variation for every alternative design, the indices in equations (5) to (7) are used as in [15]. These indices provide information about the form of building lateral displacements, whether they are shear-type or flexural-type dominated. Index ρ_i is defined as the ratio of the sum of stiffness ratio of all beams at floor i to the sum of the stiffness ratio of all columns at the same floor. When ρ_i equals to zero, then pure flexural-type deformation occurs and if ρ_i becomes infinite then pure shear-type deformation occurs, while intermediate values stand for a combination of the 2 types where both beams and columns deform in flexure. Index ρ_b quantifies the variation of beams stiffness and is defined as the ratio of the sum of stiffness ratio of all beams at each floor to the sum of the stiffness ratio of all beams at the first floor. Similarly, index ρ_c is defined for columns.

$$\rho_i = \frac{\sum_{\text{story } i \text{ beams}} \frac{EI_b}{L_b}}{\sum_{\text{story } i \text{ columns}} \frac{EI_c}{L_c}} \tag{5}$$

$$\rho_b = \frac{\sum_{\text{story } i} \frac{I_b}{L_b}}{\sum_{1st \text{ story}} \frac{I_b}{L_b}} \tag{6}$$

$$\rho_c = \frac{\sum_{\text{story } i} \frac{I_c}{L_c}}{\sum_{1st \text{ story}} \frac{I_c}{L_c}} \tag{7}$$

In Figure 10, all the above indices are presented for the 3 frames designed to have different stiffness variation along height. Frame (a) is the 6-storey, 2-bay frame presented in §(3.1). This frame is designed according to Greek codes with variation in columns reinforcement along height. External columns maintain the same amount of reinforcement, while the interior ones reduce steel bars diameters in the 5th and 6th floor. Frame's (b) reinforcement remains constant along height in each column so as in all storeys its index ρ_i to take approximately the same mean value with frame (a). Frame (c) is based on frame (b), but with beam cross sections varying as number of floor increases. This variation is applied only in cross sections and not in the reinforcement so as yield moment strength to remain practically constant.

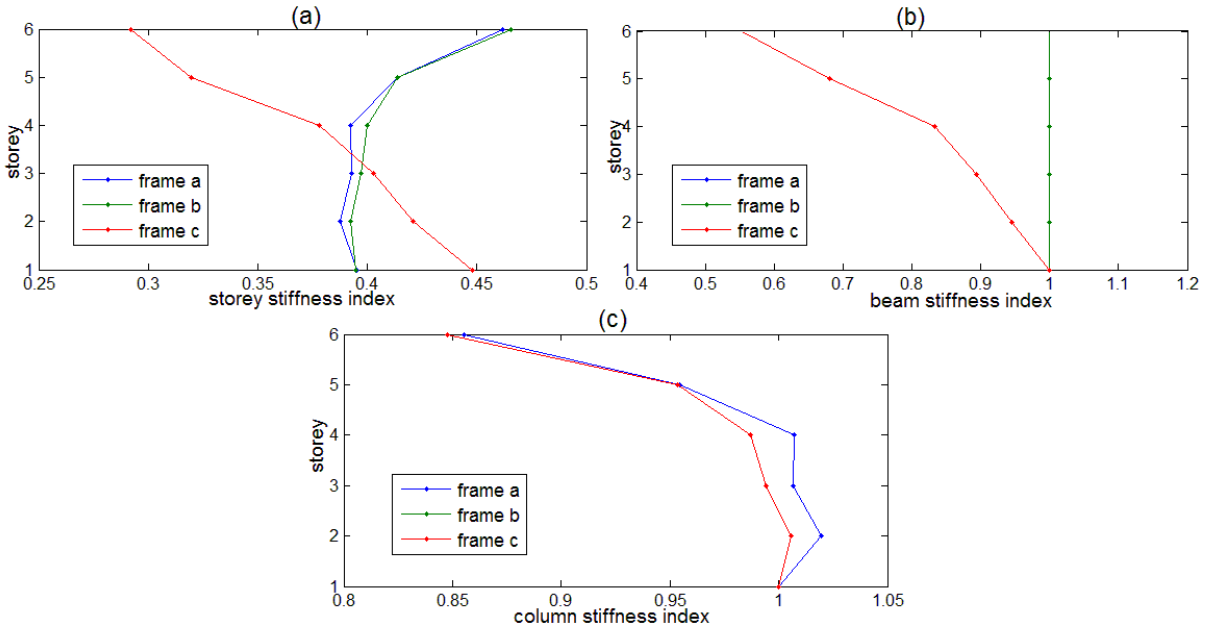

Figure 10: Variation of stiffness along height for the 3 alternative designs. a) Storey stiffness index ρ_i , b) Beam stiffness index ρ_b , c) Column stiffness index ρ_c

In the first two frames, that present constant beam stiffness in all storeys, ρ_i index attains

bigger values in upper floors as reinforcement in columns decreases. On the other hand with beam cross section reduction in size in the 3rd design, index ρ_b becomes smaller as presented in Figure 10b. In the same figure, plots for frames (a), (b) are identical as their beams are the same everywhere, while in Figure 10c, plots for frames (b), (c) are identical as they have the same column properties. In general, variation of beam moments of inertia affects the frames in which beams rotations influence their deformation more than columns lateral displacements.

After performing IDA for the three frames, fragility curves are determined which are presented in Figure 11. Intuitively, one would expect that equal stiffness in each storey would have forced damage to concentrate on lower floors, dictating the collapse capacity to decrease. However, as it is portrayed in Figure 11, using the same amount of reinforcement in columns results into slight augmentation of collapse spectral acceleration. Nevertheless, there is no more collapse capacity increase when beam cross sections vary while keeping the reinforcement and the cross section of columns constant.

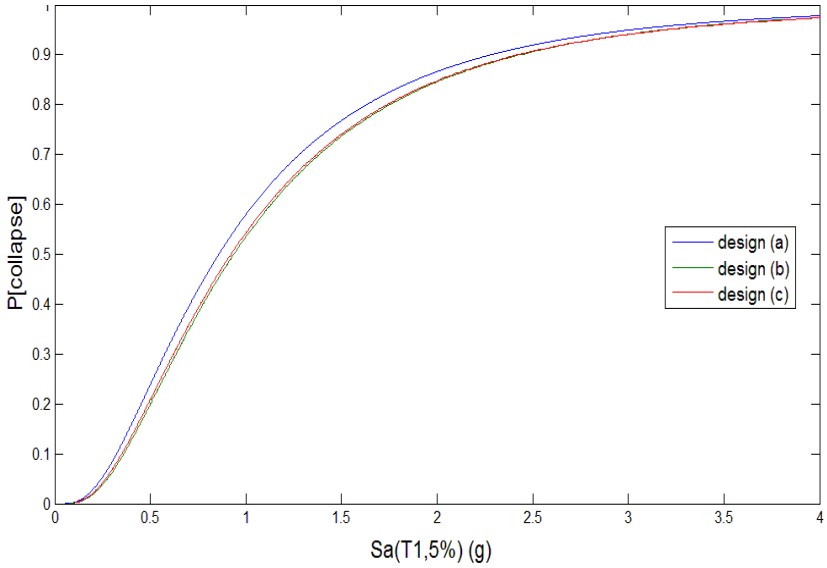

Figure 11: Fragility curves of the 3 RC frames with different stiffness variation along height

Fragility behaviour is quantified through the calculation of probabilistic indices described in §(2.2). The new outcomes are presented in table 4 below.

Frame	T1(sec)	Median (Sa_C)	σ_{ln}	$P_{C\|10\%/50y}$	MAC	λ_C	Median (IDR)	Median (RDR)
a	0.693	0.86	0.76	65%	0.75	0.0078	0.080	0.035
b	0.694	0.94	0.74	61%	0.82	0.0072	0.080	0.046
c	0.705	0.93	0.75	62%	0.81	0.0072	0.076	0.035

Table 4: Collapse capacity quantification for the 3 different design alternatives

From Table 4 a significant feature based on IDR/RDR ratio is displayed, which describes damage localization in specific storeys. The smaller value for frame (b), meaning more similar damage distribution along height, is a main reason for the higher collapse capacity exhibited. This ratio is smaller because displacements in terms of roof drift ratio appears to be greater for frame (b) since it has less stiffness in its lower columns, facilitating in this way plastic hinge formation in these critical regions. Therefore, plastic hinges at the bottom of first

floor columns helps seismic energy dissipation and is a positive feature for capacity design. More specifically, plastic hinge distribution at collapse can be found in Table 5. Generally, no significant differences are observed in the way that stiffness distribution affects plastic hinge distribution. For the case of frame (b) with uniform column reinforcement, in 50% of all the occasions plastic hinges are formed up to 5th storey. Hence, it isn't the fact that more storeys are involved in collapse mechanism which increases collapse capacity, but the fact that more columns participate in the mechanism, as they aren't as stiffened as in frame (a) where lower storey columns were designed with increased reinforcement.

Percentages of observed plastic hinges							
Frames	Storeys 1-1 (%)	Storeys 1-2 (%)	Storeys 1-3(%)	Storeys 1-4(%)	Storeys 1-5(%)	Storeys 1-6(%)	Percentages of storeys involved in collapse (%)
a	0	0	15	15	35	35	82
b	0	0	15	10	50	25	81
c	0	0	15	10	45	30	82

Table 5: Storeys involved in collapse mechanism for each frame

3.3 Effect of the strong column-weak beam ratio

The aim of the strong column-weak beam (SCWB) design provision is to avoid localized story mechanisms and thus attain more distributed failure mechanisms. In order to study the effect of this concept, only yield moments of beams and columns are taken into account through index α [15], which is defined as the ratio of the sum of columns yield moments to the sum of beams yield moments that exist in a given joint.

$$\alpha = \frac{\sum M_{c,y}}{\sum M_{b,y}} \tag{8}$$

In this work, the alternative designs are based in the 3-storey, 3-bay frame, where beams reinforcement remains constant and only columns reinforcement varies from one design to another resulting in different α values. Lastly, index α is referred to the middle joint of the 1st floor.

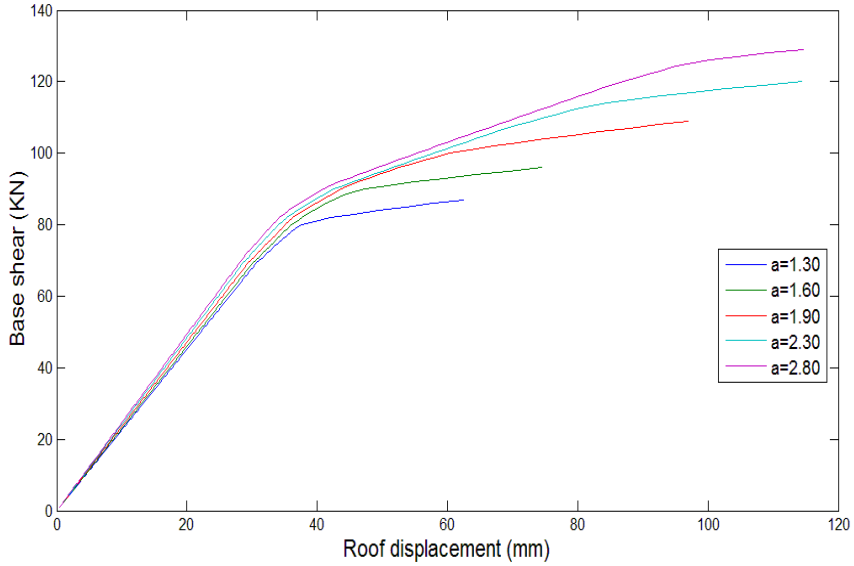

Figure 12: Static pushover curves for the different SCWB ratios

First, a static pushover analysis is performed for the five resulting RC frames and the outcome is presented in Figure 12 in order to depict the primal behaviour which will be compared with IDA. Generally, the dominant tendency is an increase of ultimate strength with the increase of column reinforcement. In addition, ductility is getting bigger and bigger up to $\alpha = 2.30$, where reinforcement area is the 2% of cross sectional area.

After performing IDA for all five frames, the fragility curves are determined which are displayed in Figure 13. Also, the accompanying probabilistic indices are included in Table 6.

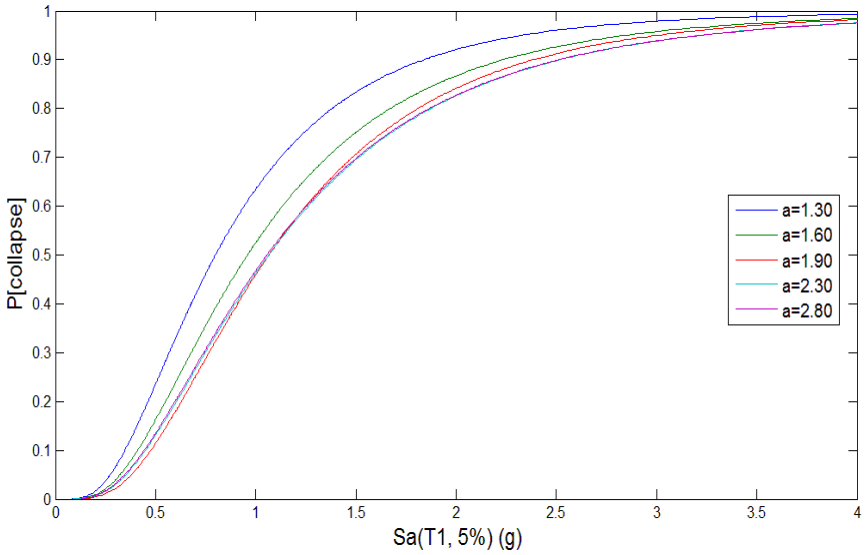

Figure 13: Fragility curves for the different SCWB ratios

α	T1(sec)	Median (Sa_C)	$\sigma_{\ln}$	$P_{C\|10\%/50y}$	MAC	λ_C	Median (IDR)	Median (RDR)
1.30	0.386	0.80	0.65	77%	0.62	0.0133	0.052	0.032
1.60	0.375	0.96	0.66	68%	0.74	0.0109	0.069	0.048
1.90	0.368	1.07	0.63	62%	0.82	0.0098	0.066	0.049
2.30	0.365	1.07	0.67	62%	0.82	0.0097	0.076	0.056
2.80	0.363	1.06	0.68	62%	0.82	0.0097	0.077	0.056

Table 6: Collapse capacity quantification for the 5 different SCWB ratios

The results in Figure 13 and Table 6 present increased collapse strength until $\alpha = 1.90$ and after that, further increase in α does not result into bigger collapse capacity, as fragility curves for $\alpha = 2.30$ and $\alpha = 2.80$ slightly differ from the fragility curve for $\alpha = 1.90$. Actually, due to larger dispersion in the last two cases, these curves present smaller collapse spectral accelerations at low collapse probabilities. Therefore, a difference in results is observed in comparison with pushover, since collapse capacity doesn't increases repeatedly when more reinforcement is added in columns. However, IDA defines a strength limit that can be assessed, meaning that the addition of more reinforcement in columns has no effect except the increase in cost. For the case of the frame studied here, this limit is accessed for $\alpha = 2$, when yield moment of columns is twice the yield moment of beams.

The results of Table 6 are displayed graphically in Figure 14. Both from Table 6 and figure 14 it is evident that there is an improvement by 15% in collapse capacity from the worst to the best design. Also an improvement of 33% at median collapse spectral acceleration and at the margin against collapse occurs, while the return period of collapse increases by 28 years. In terms of displacements, frame exhibits repeatedly larger interstorey

and roof drifts up to $\alpha = 2.30$, while for $\alpha = 2.80$ no further increase occurs, which is in agreement with the static pushover results. In order to elaborate on the fact that improvement of collapse capacity is bounded up to a certain level, the results of plastic hinge formation during formation of collapse mechanisms are listed in Table 7.

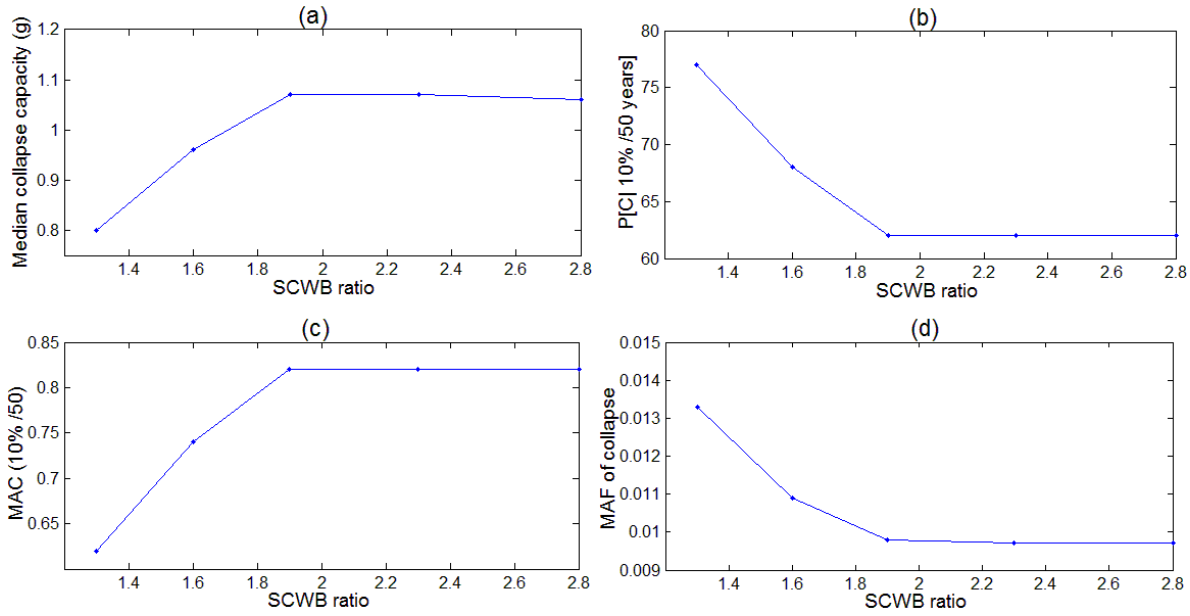

Figure 14: Effect of SCWB ratio on collapse capacity for a 3 storey, 2 bay RC frame

α	Average number of plastic hinges formed (%)	Plastic hinges percentages at columns (%)	Plastic hinges percentages at beams (%)	Capacity design violation percentages (%)
1.30	19.5	57	43	55
1.60	21	45	55	45
1.90	21	33	66	15
2.30	19.5	20	80	15
2.80	18	12	88	5

Table 7: Plastic hinge percentages at collapse

In the last column of Table 7, capacity design violation is considered to occur when a column fails prior to a beam at a given joint in the structure. Such violation can happen even if the formation of a plastic hinge at a beam isn't adequate to prevent final failure at column in the joint. As expected, more plastic hinges are formed in beams as column flexural strength increases, while the average number of total plastic hinges formed remains unaffected with SCWB ratio, meaning that only distribution of plastic hinges changes. Also, violation of capacity design regulation percentages are reduced while this ratio gets bigger. However, for values larger than 1.90 this percentage doesn't appear to differ a lot, a fact that is also portrayed by the similarity of fragility curves presented in Figure 13. Thus, it is clear that when capacity design provisions are robust, then an optimum design with respect to the probability of collapse can be achieved.

It must also be stated that an even better design can be assessed combining both beam and column flexural strength in the process and not just the SCWB ratio. Indicatively, in Figure 15 two fragility curves are presented which represent the same frame with $\alpha = 2.30$ and an alternative design where beams yield moment improved with the ratio α becoming 1.75. It is

clear that this transformation increases slightly collapse capacity by increasing beam rotational capacity, justifying the claim that total structural strength is not affected only by the SCWB ratio but also by the member's strength.

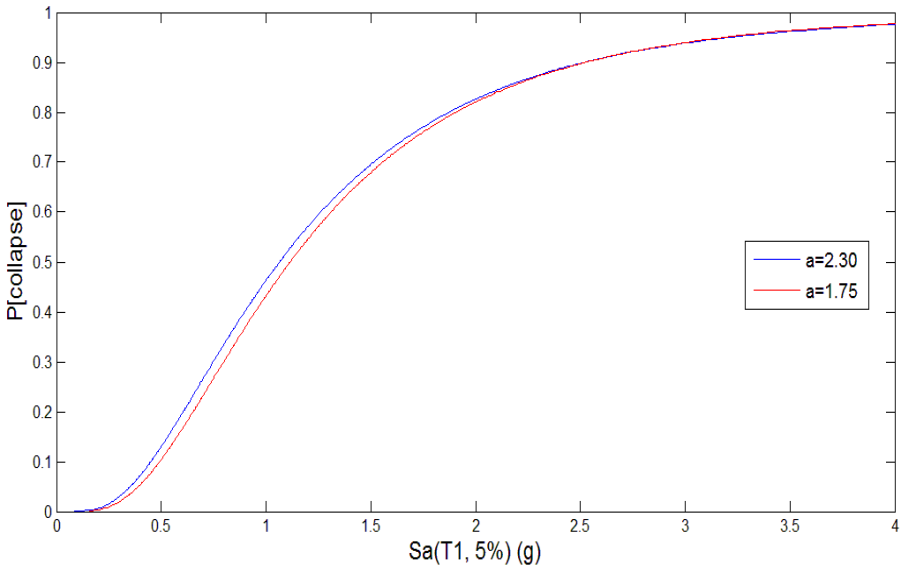

Figure 15: Fragility curves for the same frame after reducing α through beam yield moment increase

4 CONCLUSIONS

In this work fragility curves following IDA have been determined for a series of 2D RC frames to estimate the effect on their collapse capacity when some of their properties are changed. The main remarks drawn can be summarized as follows:

- For the set of frames studied in this work IDA offers similar results with pushover analysis. However, pushover analysis predicts larger differences between results in collapse capacities.
- By calculating mean values for the two groups of frames concerning 6 and 3-storey frames, 17% reduction in collapse probability assuming the 10% in 50 years earthquake occurs and 28% reduction in terms of MAF of collapse achieved when number of bays increased from 1 to 4.
- When stiffness distribution along height varies, probability of collapse reduced only 3% and MAF of collapse improved by 8%.
- With regard to the SCWB ratio, probability of collapse becomes 15% lower, while MAF of collapse is reduced by 27%. Also, it was found that there is an upper limit beyond which collapse capacity is not improving.
- By quantifying the sensitivity in collapse capacity with respect to the investigated factors, it can be concluded that the major factor is redundancy of the structure which is affected by adding more bays. Of equal importance is the SCWB ratio that affects the form of collapse mechanism throughout the structure. Stiffness distribution along the height of the structure appears to be insignificant, suggesting constant reinforcement along the height.
- More elaborate analysis should be performed to establish more general results which should be based on more representative samples and further variation of parameters.

REFFERENCES

[1] D. Vamvatsikos and A. Cornell, *Incremental Dynamic Analysis, Earthquake Eng. Struct. Dyn.* **31** (3), 491–514.

[2] D. Vamvatsikos and A. Cornell, *Applied Incremental Dynamic Analysis, Earthquake Spectra,* Volume 20, No. 2, pages 523–553, May 2004.

[3] F. Jalayer and A.Cornell, *A Technical Framework for Probability-Based Demand and Capacity Factor Design (DCFD) Seismic Formats, PEER Report* 2003/08, November 2003.

[4] F. Zareian, H. Krawinkler, L. Ibarra and D. Lignos, *Basic concepts and performance measures in prediction of collapse of buildings under earthquake ground motions, Struct. Design Tall Spec. Build.* **19***,* 167–181.

[5] Chatzi, E.N., Triantafillou S.P. and Koumousis V.K., *A computer program for 3D inelastic analysis of R/C structures*, *5th GRACM International Congress on Computational Mechanics*, Limassol, July, 2005.

[6] Charalampakis, A.E., Koumousis, V.K., (2008), *Identification of Bouc-Wen hysteretic systems by a hybrid evolutionary algorithm, Journal of Sound and Vibration,* doi:10.1016/j.jsv.2008.01.018.

[7] E.L. Wilson and A. Habibullah, *Static and Dynamic Analysis of Multi – Story Buildings, Including P-Delta effects, Earthquake Spectra, Earthquake Engineering Research Institute* Vol. 3, No. 2, May 1987

[8] D. Vamvatsikos, F. Jalayer, A. Cornell, *Application of Incremental Dynamic Analysis to an RC – Structure, FIB symposium on concrete*, 2003.

[9] H. Krawinkler, R. Medina, B. *Alavi, Seismic drift and ductility demands and their dependence on ground motions, Engineering Structures* **25** (2003) 637–653, 2003.

[10] R. A. Medina and H. Krawinkler, *Seismic Demand for Nondeteriorating Frame Structures and their Dependence on Ground Motions*, Report No. 144, *John A. Blume Earthquake Engineering Center*, December 2003.

[11] C. Haselton, G. Deierlein, *Assessing Seismic Collapse Safety of Modern Reinforced Concrete Moment-Frame Buildings, PEER Report* 2007/08, February 2008.

[12] A. Liel, C. Haselton, G. Deierlein, J. Baker, *Incorporating Modeling Uncertainties in the Assessment of Seismic Collapse Risk of Buildings, Structural Safety* **31** (2009) 197-211.

[13] M.M. Manola, V. Koumousis, *The Role of Redundancy and Overstrength in Earthquake Resisting Design, 9th International Congress on Mechanics* Limassol, Cyprus, July 2010.

[14] Bertero, R. D., and Bertero, V. V. (1999), *Redundancy in earthquake-resistant design, J. Struct. Eng*., **125** (1), 81-88.

[15] F. Zareian, H. Krawinkler, *Simplified Performance Based Earthquake Engineering*, Report No. 169, *John A. Blume Earthquake Engineering Center*, April 2009.

[16] F. Zareian, H. Krawinkler, *Structural System Parameter Selection Based on Collapse Potential of Buildings in Earthquakes*, *Journal of Structural Engineering* ASCE/ August 2010/ **933.**